

# Hybrid Telemetric MEMS for High Temperature Measurements into Harsh Industrial Environments

D. Marioli, E. Sardini, M. Serpelloni  
Dip. di Elettronica per l'Automazione  
University of Brescia  
V. Branze 38, 25123 Brescia, Italy  
mauro.serpelloni@ing.unibs.it

B. Andò, S. Baglio, N. Savalli, C. Trigona  
Dip. di Ingegneria Elettrica, Elettronica e dei Sistemi  
University of Catania  
V. Andrea Doria 6, 95125 Catania, Italy

**Abstract** – A temperature sensor that could be interrogated contactless represents an attractive solution for measurements into harsh environments such as in presence of high temperatures that do not permit the correct working of electronics. This paper discusses a telemetric system consisting of two coupled planar inductors, which constitute a coupled transformer with the primary one connected to the measurement electronics and the secondary one to a capacitive MEMS sensor that is designed for high-temperature environments. The proposed hybrid sensor is composed by the capacitive MEMS bonded to the planar inductor. The hybrid sensor behaves as an LC resonant circuit in which the MEMS represents the capacitance and the planar inductor is the inductance. The whole system has been tested in the laboratory and several results are reported. The proposed telemetric temperature system can be a solution for efficiency monitoring and predictive maintenance for harsh and complex environments.

**Keywords** - High Temperature Measurement; Wireless System; MEMS; Contactless Telemetric System; Predictive Maintenance; Process Control.

## I. INTRODUCTION

High temperature measurements are required in several industrial applications such as process control, safety evaluation, reliability prediction, product liability, and quality control. Some harsh environments are high temperature rooms, industrial ovens, rooms dedicated to experiments involving ionizing radiations. Moreover, in several applications there is the necessity to maintain a hermetic environment, such as in controlled drying processes and pressurized fluids. In these cases, the environment is unsuitable for the commercial electronic circuits that do not work in presence of temperatures greater than 100 °C; thus, the measurement system is often divided by two subsystems one of which is the sensitive element constituted by a passive probe, such as RTD, thermocouples or optical fiber [1]. The sensing element is positioned into the harsh environment, while the second part of the measurement system consisting of all the active devices of the conditioning electronics required to extract the measurement information is outside in a safe zone. In fact, the readout part works at fewer temperatures, which are compatible with the specific requirements of the active devices. Usually the two subsystems are connected by wires or optical fibers, requiring a direct link between the safe and harsh zones.

In some cases, the harsh environment is hermetic as well, for security purpose or functioning requirement, and in this case, a direct hardware connection between the probe and the conditioning electronics is not possible. Optical instruments such as pyrometers or IR optic sensor sometimes offer a solution. In [2] a novel ceramic MEMS technology based on the application of thin alumina film for high-temperature gas sensor is discussed. The MEMS platform demonstrates very high stability at working temperatures up to 600 °C. In this IR optic (NDIR) sensor, the measured value is the reduction of the intensity of IR radiation due to its absorption by a target gas. They represent well-accepted non-contact temperature measurement devices, even if they require a transparent material between them and the measurement point. Furthermore, high-temperature sensors that use surface acoustic waves (SAWs) are attractive. In [3], a wireless sensor based on (SAW) is presented. The SAW operates completely passive; interrogation is done in frequency-domain based on radar principles. Temperature range is guaranteed up to 400 °C. In [4] a contactless ultrasonic sensor based on SAW is described. A complete optical system for generating and detecting surface acoustic waves in metal versus temperature up to melting point is performed. Many applications of contactless temperature measurements is often made with radiometric surface thermometers commonly referred to as infrared thermometer for a lower range of values. Infrared thermocouples are widely available and often used in agriculture research: a typical measurement range of a consumer-quality IR thermometer is about -33 to 200 °C [5]. Furthermore, magnetic coupling between the sensor and the transducer [6] constitutes the contactless measurement. The temperature sensor is the NiFe alloy that is strongly temperature dependant. The experiments were carried out in a range from room temperature up to 90 °C.

A telemetric system represents an interesting solution for connecting the probe positioned into the hazardous zone with the conditioning electronics in the safe zone. Moreover, they represent a viable solution when the measurement environment is contained into an enclosed and hermetic space and the required wire-link through the separating wall, between the harsh and safe zones, is not possible due to the presence of high pressure or to the use of expensive connecting techniques. In

literature, telemetric systems are applied in industrial fields, for example, when the measuring environment is not accessible, since it is inside a hermetic environment [7, 8, 9]. In [7] the telemetric system is used to monitor the pressure inside a high temperature environment. The sensing technique is based on a change of the resonant frequency of a LC circuit depending on the sensor capacitance. Other examples of a passive telemetric system for chemical monitoring are quoted in [10-11]. In [12] a passive wireless temperature sensor operating in harsh environment for high-temperature rotating component monitoring is reported. The novel high-k temperature sensitive ceramic material has been developed to work up to 235 °C. The temperature sensor is composed of a ceramic multi-layer capacitor integrated with planar inductor, which forms an LC resonant circuit.

In this paper, a telemetric system is proposed for the measurement of high temperatures in harsh industrial environments. A novel MEMS temperature sensor connected to a planar inductor, which is realized in thick film technology, constitutes the sensitive element. The common working principle of the MEMS sensor is based on the structural deformation that appears as consequence of a temperature increase. A temperature sensor with several designs, fabrications and testing procedures of micro fabricated temperature sensors have been presented in literature [13], with different architectures [14]. The proposed hybrid MEMS sensor is composed by a cascade of bent beam structures in order to enhance the sensitivity of the sensor [15]. To acquire the temperature value, different measurement techniques are reported. Almost all are based on impedance measurements, to identify a particular resonant frequency, or a frequency point that has a particular property such as a minimum of the phase, or to compensate the distance changes through the measurement of three resonance frequencies. An electronic circuit suitable for the characteristics of the hybrid MEMS telemetric measurement system is under analysis and development. To experimentally verify the characteristics of the proposed measurement system, a telemetric apparatus consisting of a hybrid sensor and a readout inductor have been preliminary tested into a temperature-controlled measurement oven. The reported experimental results have been measured with the aid of an impedance analyzer.

## II. TELEMETRIC SYSTEM

The proposed telemetric system is reported schematically in Figure 1: on the left the hybrid telemetric MEMS is placed into the harsh environment, while, on the right, the conditioning electronics is into the safe zone. A wall separates the two zones and the two subsystems communicate through a magnetic field. This wall has no magnetic or conductive properties so that guarantees the magnetic coupling. In industrial ovens a thin separation wall made by temperate glass are used for visual inspection of the internal process. The small area and the thermal and physical settings of these glasses guarantee low heat dispersion; thus, the temperature inside the oven is uniform to the one near the wall. The images of the two inductors called “sensing inductor” and “readout inductor” are reported in Figure 1, as well.

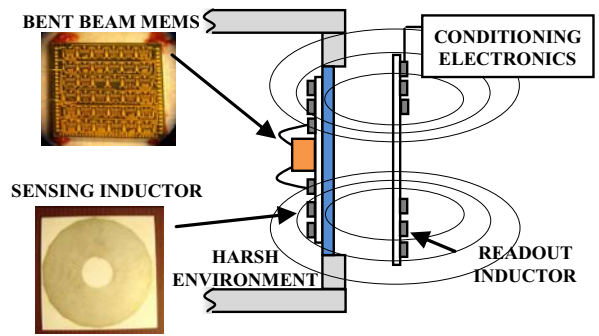


Figure 1. Block diagram of the telemetric system.

### A. Hybrid Telemetric MEMS

The hybrid telemetric MEMS placed inside the harsh environment is composed by a novel MEMS temperature sensor developed using the Metal MUMPs process [15] and a planar inductor with high-temperature characteristics. The capacitive MEMS is positioned centrally to the inductor and bonded to it (Figure 2). The hybrid telemetric MEMS behaves as an LC resonant circuit in which the MEMS represents the capacitance and the planar inductor is the inductance. The MEMS sensor is based on a cascade of bent beam structures. The single structure is composed by a V-shaped beam anchored at two ends as reported in Figure 3. The temperature variation induces a thermal expansion of the structure generating a displacement of the central apex, which is connected to an interdigitated comb. The device is built directly over a silicon nitride isolation layer with a 1 μm air gap, or over a 25 μm deep trench, which is etched into the substrate. The maximum operating temperature is due to the maximum operating limit of nickel (350 °C).

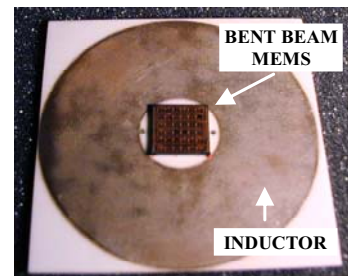


Figure 2. Image of the hybrid telemetric MEMS.

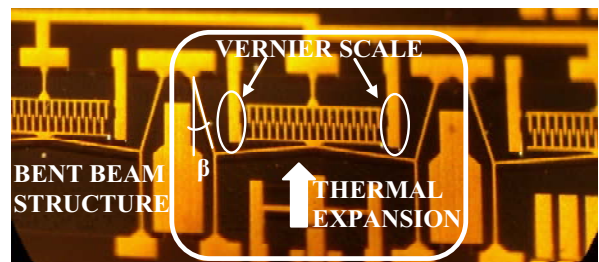


Figure 3. Image of a bent beam structure.

The prototypes have been made relatively big, since the minimum line width and space for the nickel structural layer is

8  $\mu\text{m}$ . The realized prototype has a beam's length of 500  $\mu\text{m}$ , beam's width of 10  $\mu\text{m}$ ,  $\beta=7^\circ$  (Figure 3).

The following equation has been used to derive the analytical values of the sensor as a function of temperature:

$$C'_S = 2N_r \epsilon_0 \frac{(y_0 + y)}{x_0} t \quad (1)$$

Where  $N_r$  is the number of fingers of the moveable electrode,  $y_0$  the initial overlap between fingers,  $y$  the displacement dependent on temperature,  $x_0$  the lateral gap between finger,  $t$  the nickel thickness and  $\epsilon_0$  the vacuum permittivity. As shown in Figure 3, two Vernier scales have been positioned to evaluate the deformations during the characterization.

Several inductors have been fabricated exploiting two different technologies. In Table I the characteristics of the fabricated inductors are reported. The planar inductors A1 and A2 are obtained using thick-film technology by screen printing and micro-cutting by a laser-beam. During the screen printing two conductive (QM14 commercialized by Du Pont) films, one overlapping the other, were deposited to reach a thickness of about 20  $\mu\text{m}$  over an alumina substrate (50x50x0.63 mm). The conductive film has a resistivity of about 1.5-2.5 m $\Omega$ /sq. The deposited film was dried for 10-15 minutes at 150  $^\circ\text{C}$  and then was fired in a conveyor furnace for 30 minutes with a peak temperature of 850  $^\circ\text{C}$ . The micro-cutting process consists of material erosion operated by a laser-beam. The inductors have the external diameter of 50 mm, 120 windings each of about 89  $\mu\text{m}$  width and spaced 75  $\mu\text{m}$  from the others (Figure 4).

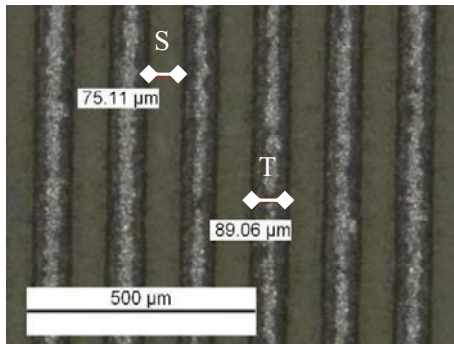


Figure 4. Microscope image of the inductor A1 realized by thick film deposition on alumina.

A second set of planar inductors was realized by a photolithographic technology on a substrate operating at high-temperature. The adopted 85N polyimide laminate is commercialized by Arlon and has a good resistance to high temperature (up to 280  $^\circ\text{C}$ ). The substrate is a double layer laminate with copper (35  $\mu\text{m}$ ). The photolithographic process used light to transfer the spiral pattern from a photomask to a light-sensitive chemical (photoresist) on the substrate (Figure 5). A series of chemical treatments then engraves the exposure pattern into the material underneath the photoresist. The planar inductors were realized with two different patterns, as reported in Table I. The equivalent circuit parameters of every single inductor (consisting in the series of an inductance and a resistance both in parallel with a capacitance) were measured by the impedance analyzer (HP4194A) and their values are reported in Table II.

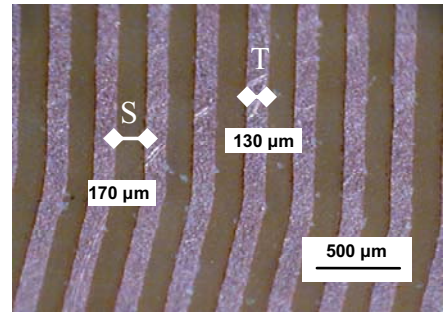


Figure 5. Microscope image of the inductor B1 realized by photolithography.

The capacitive MEMS are fixed to the sensing inductor by a high-temperature ceramic adhesive (Resbond 931C) commercialized by Cotronics. The contact pads are bonded to the inductor terminals. The hybrid telemetric MEMS were characterized at room temperature. The  $R_S$ ,  $C_S$  and  $L_S$ , respectively the resistance, the inductance and capacitance of the hybrid telemetric MEMS sensor, were measured with an impedance analyzer (HP4194A) and the results are reported in Table III. The hybrid sensor realized by the thick-film inductor A1 presents wider temperature range and lower resonant frequency, but higher resistance than the inductor B1. A high-temperature range permits a wide range of applications, while a less resistance permits to improve the quality factor of the resonance. The experimental data reported in section IV was obtained by the hybrid sensor A1. For applications with temperature up to 280  $^\circ\text{C}$  the hybrid sensor B1 could be used as well, improving the quality factor of the resonances.

TABLE I. CHARACTERISTICS OF THE PLANAR INDUCTORS.

| Inductors | Technology   | Windings | Length S [ $\mu\text{m}$ ] | Length T [ $\mu\text{m}$ ] |
|-----------|--------------|----------|----------------------------|----------------------------|
| A1        | Thick films  | 120      | 75                         | 89                         |
| A2        | Thick films  | 120      | 75                         | 89                         |
| B1        | Photolithog. | 75       | 170                        | 130                        |
| B2        | Photolithog. | 110      | 110                        | 90                         |

TABLE II. EQUIVALENT CIRCUIT PARAMETERS OF THE INDUCTORS.

| Inductors | Inductance ( $\mu\text{H}$ ) | Capacitance (pF) | Resistance ( $\Omega$ ) |
|-----------|------------------------------|------------------|-------------------------|
| A1        | 335                          | 1.35             | 170                     |
| A2        | 340                          | 1.32             | 175                     |
| B1        | 82                           | 1.2              | 51                      |
| B2        | 138                          | 1.1              | 96                      |
| Readout   | 14.5                         | 91.4             | 20                      |

TABLE III. EQUIVALENT CIRCUIT PARAMETERS OF THE HYBRID SENSORS.

| Hybrid sensors | Inductance ( $\mu\text{H}$ ) | Capacitance (pF) | Resistance ( $\Omega$ ) |
|----------------|------------------------------|------------------|-------------------------|
| Hybrid A1      | 235.2                        | 19.5             | 172                     |
| Hybrid B1      | 69.3                         | 18.2             | 51                      |

### B. Measuring circuit

The readout device is composed by a readout inductor connected to a conditioning electronics. The readout inductor is a planar spiral fabricated in thick-film technology and it has 30 windings, each of 250  $\mu\text{m}$  width and spaced 250  $\mu\text{m}$  from the others. The external diameter is 50 mm wide. The impedance measured by an impedance analyzer (HP4194A) as seen from the terminals of the readout inductor shows in Figure 6 the three resonant frequencies ( $f_{ra}, f_{rb}, f_a$ ).

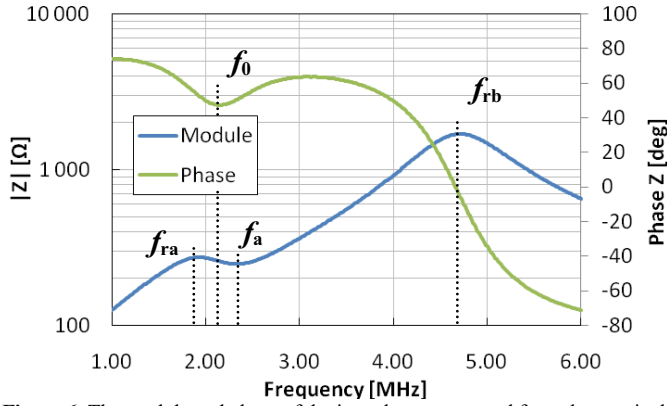


Figure 6. The module and phase of the impedance measured from the terminals of the readout inductance.

In literature different measurement techniques suitable to obtain the MEMS capacitance are reported. They are based on impedance measurements: a resonant frequency or a frequency that has a particular property such as a minimum of the phase of the impedance is measured (Min-Phase method [7]). In [16] three resonance frequencies are measured with the aim to calculate the sensor capacitance and to compensate the distance variations (3-Resonances method). According to [16], the capacitive value of the MEMS sensor is obtained as the product among a constant term  $k$  and one calculated by the measures of  $f_{ra}, f_{rb}, f_a$ , as reported in equation 2.

$$C'_S = k \frac{(2\pi f_{ra})^2 + (2\pi f_{rb})^2 - (2\pi f_a)^2}{(2\pi f_a)^2} \quad (2)$$

$$k = \frac{L_1 C_r}{L_2} \quad (3)$$

The constant term  $k$  can be obtained automatically by calibration, or calculated by measuring the parameters of the equivalent circuit of the readout inductor and the hybrid sensor, where  $L_1$  and  $L_2$  represent the inductance values of the readout and sensing and  $C_r$  is the parasitic capacitance of the readout inductor. The equivalent circuit parameters consisting in the series of an inductance and a resistance both in parallel with a capacitance, were measured by the impedance analyzer (HP4194A) and its values are  $L_1$  of about 14.5  $\mu\text{H}$ ,  $C_r$  of about 91.4 pF. The equivalent circuit parameters of the hybrid sensor are reported in Table III.

The Min-Phase method measures the impedance of the terminals of the readout inductor, as well; thus, the capacitive value of the sensor is related to the frequency at which the phase, in a short frequency interval, is at its minimum value; this frequency approximately corresponds to:

$$f_0 = \frac{1}{2\pi\sqrt{C_S L_S}} \quad (4)$$

With  $C_S$  and  $L_S$  the inductance and capacitance of the hybrid telemetric MEMS sensor. The conditioning electronics is under development according to the final characteristics of the system.

### III. EXPERIMENTAL SETUP

An experimental setup has been designed to test the telemetric measurement system at high temperatures. In Figure 7 a block diagram of the experimental setup is reported.

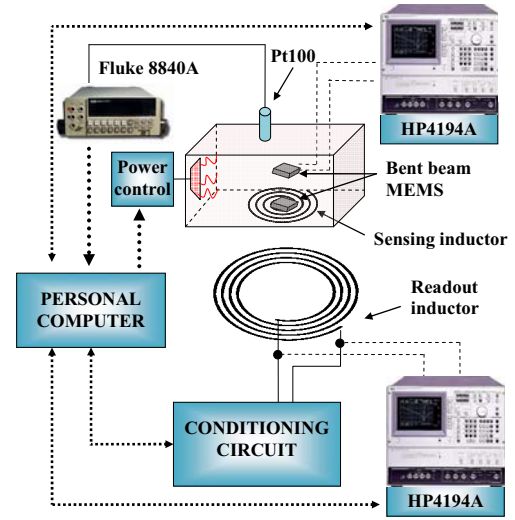


Figure 7. Block diagram of the experimental setup.

The measurement chamber is made of two walls: the internal one of aluminum and the external of steel; between them a thermo-resistive wool (Superwool607<sup>TM</sup> commercialized by Thermal Ceramics) is interposed. The total thickness of the measurement chamber is about 3 cm and the maximum space of the chamber is 30x30x13 cm. In one side a window for visual inspection of the internal process was realized by a temperate glass with a maximum working temperature of about 500 °C. The window is a square of 12x12 cm. Inside the chamber an IR heater of 500 W was mounted, permitting to reach a controlled temperature over 350 °C. Three thermo-resistances (Pt100) measure the internal temperature in three different points, each one is connected to a multimeter (Fluke 8840A). The three values are used to assure that the temperature is distributed uniformly. During the execution of the test, the thermoresistance difference of about two tens of ohms that corresponds to less than 1 °C was observed. A personal computer, running a developed LabVIEW<sup>TM</sup> virtual-instrument, is connected to the multimeters through an IEEE 488 bus and to the input of the power control through the digital output of the I/O board. The PC monitors the temperature inside the oven and controls the IR heater by turning on and off alternatively the power circuit. Furthermore, the PC controls the impedance analyzer saving and analyzing the data.

The hybrid sensors were tested into the oven. Initially one hybrid sensor was connected directly to an impedance analyzer (HP4194A) for a direct measurement of the sensor capacitance and then another hybrid sensor was used for telemetric measurements. Externally the readout inductor was connected to the input terminal of an impedance analyzer (HP4194A).

In Figure 8, the temperatures of the three thermo-resistances were monitored during a thermal cycle of heating and cooling. The diagram shows inertia in the heating process that is fast at low temperatures and slow at high temperatures. The cooling process is obtained by heat dispersion, stabilizing the temperature by the IR heater.

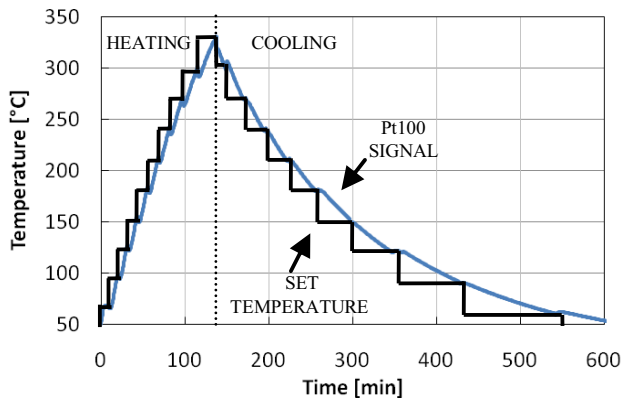


Figure 8. Temperature inside the oven as a function of time for a heating and cooling process.

#### IV. EXPERIMENTAL RESULTS

As previously reported, the impedance analyzer HP4194A is connected to the readout inductor to evaluate the telemetric system behavior, and directly to the hybrid sensor to measure, as reference, the impedance of the sensor.

The impedance of the hybrid sensor was obtained changing the temperature from about 50 °C to 330 °C with steps of 10/20 °C. The impedance analyzer (HP4194A) was set to measure module, phase and the equivalent circuit parameters (inductance, capacitance and resistance) of the device under test for every temperature steps. The sensor response was measured for different frequencies and temperatures, several results are reported in Figure 9.

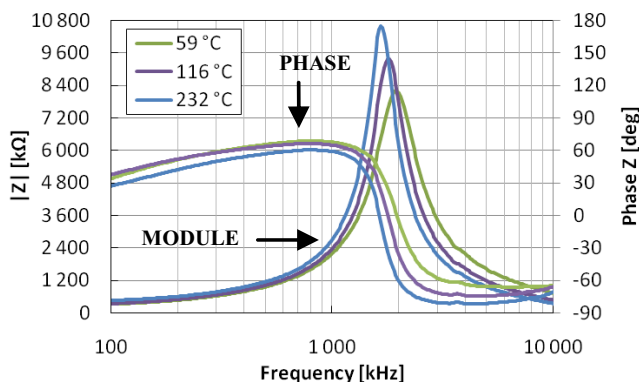


Figure 9. The impedance of the hybrid sensor for different temperatures.

Furthermore, the readout inductor was positioned axially to the hybrid sensor at about one centimeter to the hybrid sensor inside the chamber, while outside the readout was connected to the impedance analyzer. In fact, the two different methods, reported in the previous paragraph, use impedance diagrams to calculate the sensor capacitance. In Figure 10 module (a) and phase (b) diagrams of the impedance for several temperatures are reported. The diagrams are reported for a range of frequencies in which the resonant frequencies ( $f_{ra}$ ,  $f_0$ ,  $f_a$ ) are visible. As expected an increasing in temperature generates a decreasing of the values of the resonant frequencies.

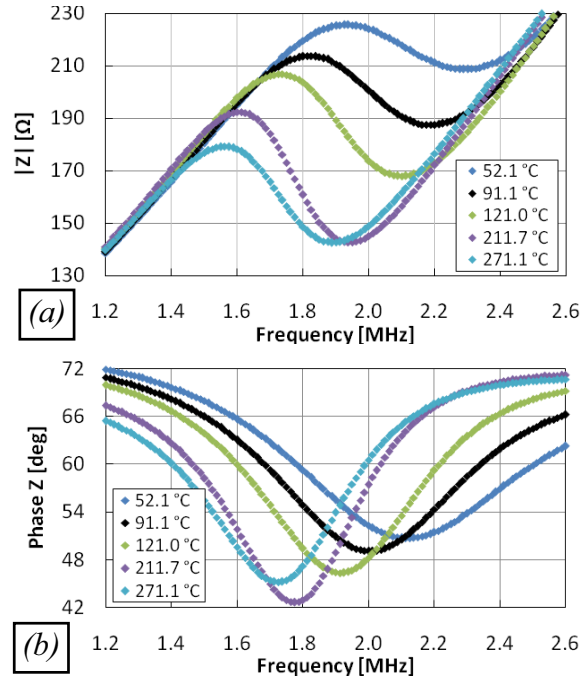


Figure 10. Module (a) and phase (b) diagrams measured with the impedance analyzer.

In Figure 11 the values of the sensor capacitance obtained by the direct measurements of the impedance are compared for different temperatures with the values calculated by the impedance diagrams using the Min-Phase and the 3-Resonances techniques. Figure 11 shows a quasi-linear behavior of the sensor. The linear polynomial interpolations are reported in Figure 11 as well. The values calculated are closely to the reference one measured with the impedance analyzer. Moreover, the capacitance values calculated completely match the reference ones for the middle temperature, while they defer in the lowest and highest range. The results reported in Figure 11 show a sensitivity of about 60 fF/°C.

In Figure 12 the temperatures measured with the reference sensor (Pt100) are compared with the values calculated by the Min-Phase and 3-Resonances methods. The temperature values are obtained using the polynomial interpolation equations reported in Figure 11. The diagrams show a good agreement of the data during both the heating and the cooling process.

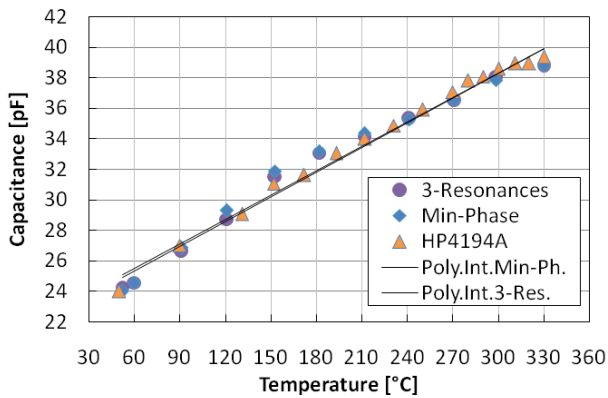


Figure 11. Capacitance sensor values directly measured and compared with the calculated ones.

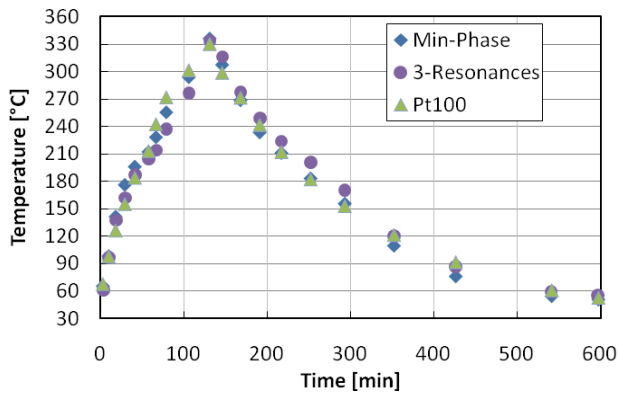


Figure 12. Temperature values measured directly and compared with the calculated ones.

## V. CONCLUSIONS AND OUTLOOK

In this paper a new hybrid telemetric MEMS for high temperature measurements has been proposed. It consists of a planar inductor bonded to a MEMS sensor. The hybrid sensor behaves as an LC resonant circuit, in which the MEMS represents the capacitance and the planar inductor is the inductance. The telemetric system consisting of one planar inductor positioned outside the harsh environment, coupled with the hybrid sensor, has been characterized. The two inductors constitute a coupled transformer with the readout one connected to the measurement electronics and the secondary one to the capacitive MEMS sensor that is designed for high-temperature environments. Two different measurement techniques have been evaluated. An experimental setup has been designed to test the hybrid sensor at high temperatures. The whole system has been characterized in the laboratory and several results are reported for a temperature up to 330 °C. The values measured by the two techniques show a good agreement with the reference ones during both the heating and the cooling process. The proposed telemetric system exploits the possibility to measure the temperature inside harsh and hermetic environments and the experimental results show good agreement. One of these techniques can be used in applications where the distance can change. A conditioning electronics is under development and will be soon available.

## REFERENCES

- [1] M. V. P. Kruger, M. H. Guddal, R. Belikov, A. Bhatnagar, O. Solgaard, C. Spanos, K. Poolla, "Low Power Wireless Readout of Autonomous Sensor Wafer using MEMS Grating Light Modulator", *Optical MEMS, 2000 IEEE/LEOS Int. Conf.*, pp. 67-68.
- [2] A.A. Vasiliev, R.G. Pavelko, S.Yu. Gogish-Klushin, D.Yu. Kharitonov, O.S. Gogish-Klushina, A.V. Sokolov, A.V. Pislakov, N.N. Samotaev, "Alumina MEMS platform for impulse semiconductor and IR optic gas sensors", *Sensors and Actuators B* 132, 2008, pp. 216-223.
- [3] A. Stelzer, S. Scheibhofer, S. Schuster, R. Teichmann, "Wireless sensor marking and temperature measurement with SAW-identification tags", *Measurement* 41, 2008, pp.579-588.
- [4] C. Hubert, M.-H. Nadal, G. Ravel-Chapuis, R. Oltra, "Contactless ultrasonic device to measure surface acoustic wave velocities versus temperature", *Review Of Scientific Instruments* 78, 2007, pp.024901-6.
- [5] J. R. Mahana, K. M. Yeater, "Agricultural applications of a low-cost infrared thermometer", *Computers and Electronics in Agriculture* 64, 2008, pp.262-267.
- [6] D. Mavrudieva, J.-Y. Voyant, A. Kedous-Lebouc, J.-P. Yonnet, "Magnetic structures for contactless temperature sensor", *Sensors and Actuators A* 142, 2008 pp.464-467.
- [7] M. A. Fonseca, J. M. English, M. Von Arx, M. G. Allen, "Wireless Micromachined Ceramic Pressure Sensor for High Temperature Applications", *J. of Microel. Systems*, vol. 11, no. 4, 2002, pp. 337-343.
- [8] M. A. Fonseca, M. G. Allen, J. Kroh, J. White, "Flexible Wireless Passive Pressure Sensors for Biomedical Applications", *Tech. Dig. Solid-State Sensor, Actuator, and Microsystems Workshop*, Hilton Head Island, SC, USA, June 2006, pp. 37-42.
- [9] Y. Jia, K. Sun, F. J. Agosto, M. T. Quinones, "Design and characterization of a passive wireless strain sensor", *Measurement Science and Technology* 17, 2006, pp. 2869-2876.
- [10] E. Birdsell, M. G. Allen, "Wireless Chemical Sensors for High Temperature environments", *Tech. Dig. Solid-State Sensor, Actuator, and Microsystems Workshop*, Hilton Head Island, SC, USA, June 2006, pp. 212-215.
- [11] E. L. Tan, W. N. Ng, R. Shao, B. D. Pereles, K. G. Ong, "A Wireless, Passive Sensor for Quantifying Packaged Food Quality", *Sensors* 7, 2007, pp. 1747-1756.
- [12] Y. Wang, Y. Jia, Q. Chen, Y. Wang, "A Passive Wireless Temperature Sensor for Harsh Environment Applications" *Sensors* 8, 2008, pp. 7982-7995.
- [13] M. Suster, D. J. Young, W. H. Ko, "Micro-power Wireless Transmitter for High-temperature MEMS Sensing and Communication Applications", *The Fifteenth IEEE Int. Conf. on Micro Electro Mechanical System*, 2002, pp. 641-644.
- [14] L. H. Han, S. Chen, "Wireless Bimorph Micro-actuators by Pulsed Laser Heating", *Sensors and Actuators A* 121, 2005, pp. 35-43.
- [15] B. Andò, S. Baglio, N. Pitrone, N. Savalli, C. Trigona, "Bent beam MEMS Temperature Sensors for Contactless Measurements in Harsh Environments", *Proceedings of IEEE I2MTC 2008*, Victoria, BC, Canada, 2008, pp. 1930-1934.
- [16] D. Marioli, E. Sardini, M. Serpelloni, "An Inductive Telemetric Measurement System for Humidity Sensing", *Measurement Science and Technology* 19, 2008, pp. 1-8.